Journal of Environmental Chemical Engineering 6 (2018) 1314–1321

Contents lists available at ScienceDirect

Journal of Environmental Chemical Engineering

journal homepage: www.elsevier.com/locate/jece

Research Paper

Electrostatic interactions in virus removal by ultrafiltration membranes

Guillermina José Gentile[a,1], Mercedes Cecilia Cruz[b,c,1], Verónica Beatriz Rajal[b,c,d], María Marta Fidalgo de Cortalezzi[a,e,*]

[a] Department of Chemical Engineering, Instituto Tecnológico de Buenos Aires (ITBA), Argentina
[b] Instituto de Investigaciones para la Industria Química – Consejo Nacional de Investigaciones Científicas y Técnicas, Universidad Nacional de Salta (UNSa), Salta, Argentina
[c] Singapore Centre for Environmental Life Sciences Engineering (SCELSE), Nanyang Technological University, 60 Nanyang Drive, 637551, Singapore
[d] Facultad de Ingeniería, Universidad Nacional de Salta (UNSa), Salta, Argentina
[e] Department of Civil and Environmental Engineering, University of Missouri, Columbia, MO, 65211, United States

ARTICLE INFO

Keywords:
Ultrafiltration
Virus removal
Water disinfection
Bacteriophage PP7
Zeta potential
DLVO

ABSTRACT

Ultrafiltration membranes are increasingly used in potabilization to remove viral particles. This removal is controlled by electrostatic repulsion, attachment and size exclusion. The effect of electrostatic interaction in virus filtration was investigated. Our work included characterization of bacteriophage PP7 and polyethersulfone membrane with respect to size and surface charge; the removal of this bacteriophage at laboratory scale by ultrafiltration membrane process and the mechanism and limitations were analyzed and discussed under DLVO and XDLVO theories. A partial removal of the bacteriophage was achieved; however, enhanced separation may be achieved considering that the process is affected by the aqueous matrix. The presence of divalent cations diminished the effectiveness of the procedure as opposed to monovalent cations and species with amphoteric behavior such as bicarbonate. DLVO and XDLVO predicted the interactions studied between bacteriophage PP7 and polyethersulfone membrane.

1. Introduction

Access to safe water is a primary objective for public health policies worldwide. The reduction and inactivation of viral pathogens in natural waters is therefore a major goal to achieve, due to the intimate relationship between this kind of organisms and disease outbreaks [1]. Available treatments based on bacteriological criteria are not always effective, since viruses are more resistant and difficult to remove [2,3].

Ultrafiltration membranes, with pore size between 1 and 100 nm [4], are increasingly used in potabilization to remove viral particles and are considered a good barrier in the nanometer scale [5]. The removal of viral particles is controlled by different mechanisms, such as electrostatic repulsion, attachment and size exclusion [4–8]. The outer surface of viruses and its charge play a key role in interactions with other surfaces and the surrounding water matrix. Therefore, conditions under which viruses are prepared, purified and conserved at laboratory scale should be taken into consideration prior to assess this kind of interactions in ultrafiltration processes [9,10].

Bacteriophages are viruses that infect bacteria. Some of them have similar structure, composition and size to human enteric viruses and thus they are valuable as models or surrogates [11]. Bacteriophages PP7 [12,13], P22 [14,15], MS2 [16–18] and X174 [18] have been used in filtration, transport, adhesion and adsorption experiments.

Virus-membrane interactions in an ultrafiltration process can be modeled in the light of DLVO theory [18], which is often applied to predict colloidal stability [19,20]. Despite the widespread use of this theory, it makes assumptions (particles are dense, solid spheres with homogenous surface) that sometimes lead to failure in explaining the interactions. Extended DLVO theory is a subject of research to overcome these limitations, since it considers additional interacting forces (Born repulsion, hydration forces and Lewis acid-base forces, among others) [18].

In this work, we characterized the bacteriophage PP7 and a polyethersulfone (PES) ultrafiltration membrane with respect to size and surface charge under a broad range of relevant conditions of pH and ionic strength and evaluated the filtration mechanism and limitations under DLVO and XDLVO theories, in order to a better understanding of the removal of bacteriophages at laboratory scale by ultrafiltration.

* Corresponding author at: Department of Civil and Environmental Engineering, University of Missouri, Columbia, MO, 65211, United States.
E-mail address: fidalgom@missouri.edu (M.M. Fidalgo de Cortalezzi).
[1] Shared first authorship.

https://doi.org/10.1016/j.jece.2017.11.041
Received 17 August 2017; Received in revised form 17 October 2017; Accepted 14 November 2017
Available online 15 November 2017
2213-3437/

Nomenclature

a	Radius of the primary aggregate of viral particles (m)
A_{11}	Hamaker constant of two viral particles
A_{22}	Hamaker constant of PES membrane
A_{33}	Hamaker constant of water
A_{131}	Hamaker constant of virus particle in water (J)
A_{132}	Combined hamaker constant of virus particle and PES membrane in water (J)
C_e	Salt concentration (mol m^{-3})
C_f	Virus concentration in the feed (gene copy ml^{-1})
C_h	Hydration constant (J)
C_j	Ion concentration (mol dm^{-3})
C_p	Virus concentration in the permeate flow (gene copy ml^{-1})
e	Electron charge (C)
h	Separation between surfaces (m)
k	Boltzmann constant (J K^{-1})
K	Hydrophobic constant (J)
LRV	Log removal value
n_∞	Bulk number of ions (ions m^{-3})
N_A	Avogadro number
T	Temperature (K)
V_{AB}	Lewis acid-base interaction potential energy (J)
V_{EDL}	Electrical double layer interaction potential energy (J)
V_H	Hydration interaction potential energy (J)
V_{DLVO}	DLVO interaction potential energy (J)
V_{TOTAL}	Total interaction potential energy (J)
V_{vdW}	Unretarded van der waals interaction potential energy (J)
z	Valence of symmetrical (z-z) electrolyte
z_j	Valence of ion j including sign of charge
Φ	Reduced potential
ζ	Zeta potential (V)
θ	Contact angle of surface (°)
κ	Debye-Hückel reciprocal length (m^{-1})
λAB	Decay (Debye) length of water (m)
φ	Electrical potential (V)
$\Phi AB_{(h = h0)}$	Lewis acid-base free interaction potential energy between surfaces at contact (J m^{-2})

2. Theory

DLVO theory explains colloid stability and attachment between colloids and between colloids and surfaces, based on two predominant forces, electrical double layer repulsion and van der Waals attraction [19,20].

The electrical double layer interaction potential energy between two spherical particles can be calculated as [21]:

$$V_{EDL} = \frac{2\pi a_1 a_2 n_\infty kT}{(a_1 + a_2)\kappa^2}(\Phi_1^2 + \Phi_2^2)\left[\frac{2\Phi_1\Phi_2}{\Phi_1^2 + \Phi_2^2} ln\frac{1 + e^{-\kappa h}}{1 - e^{-\kappa h}} + ln(1 - e^{-2\kappa h})\right] \quad (1)$$

$$\Phi = \frac{ze\varphi}{kT} \quad (2)$$

$$\kappa = 2.32x10^9\sqrt{\sum C_j z_j^2} \quad (3)$$

in aqueous solution at 25 °C where V_{EDL}: electrical double layer interaction potential energy (J), a: radius of primary aggregate (m), n_∞: bulk number of ions (ions m^{-3}), k: Boltzmann constant (J K^{-1}), T: temperature (K), κ: Debye-Hückel reciprocal length (m^{-1}), Φ: reduced potential, z: valence of symmetrical (z-z) electrolyte, h: separation between surfaces (m), e: electron charge (C), φ: electrical potential (V), Cj: ion j concentration (mol dm^{-3}), z_j: valence of ion j including sign of charge.

If there is a large difference between particle sizes, the bigger one is perceived as an infinite plate, and eq. 1 will reduce to:

$$V_{EDL} = \frac{2\pi a n_\infty kT}{\kappa^2}(\Phi_1^2 + \Phi_2^2)\left[\frac{2\Phi_1\Phi_2}{\Phi_1^2 + \Phi_2^2} ln\frac{1 + e^{-\kappa h}}{1 - e^{-\kappa h}} + ln(1 - e^{-2\kappa h})\right] \quad (4)$$

The electrical surface potential (φ) is commonly approximated by the zeta potential (ζ) (potential at the shear plane) due to the impossibility to experimentally determine the first.

The attractive van der Waals interaction potential energy between two identical spherical particles can be calculated as [21]:

$$V_{vdW} = -\frac{A_{131}}{6}\left(\frac{2a^2}{h^2 + 4ah} + \frac{2a^2}{h^2 + 4ah + 4a^2} + ln\frac{h^2 + 4ah}{h^2 + 4ah + 4a^2}\right) \quad (5)$$

where V_{vdW}: unretarded van der Waals interaction potential energy (J), A_{131}: Hamaker constant for two spheres of material 1 suspended in medium 3 (J). For a sphere and an infinite plate, the following expression applies [21]:

$$V_{vdW} = -\frac{A_{132}}{6}\left(\frac{a}{h} + \frac{a}{h + 2a} + ln\frac{h}{h + 2a}\right) \quad (6)$$

where A_{132}: combined Hamaker constant for the sphere 1 and the Plate 2 in medium 3 (J).

The DLVO interaction potential energy is the sum of electrical double layer and van der Waals interactions:

$$V_{DLVO} = V_{EDL} + V_{vdW} \quad (7)$$

Additional interacting forces (Born repulsion, hydration forces and Lewis acid-base forces among others) may also exist, giving rise to the extended DLVO theory. Born short-range forces are originated from the repulsion between electrons of different atoms when their shells interpenetrate each other. However, hydrated ions, present in the medium, prevent separations between surfaces of less than 0.3 nm, and these repulsion forces can easily be neglected [18,21]. Lewis acid-base interactions arise from migration of electrons between the surfaces, adsorbed species and the solvent; and can be calculated as follows for two spheres [18]:

$$V_{AB} = 2\pi\frac{a_1 a_2}{a_1 + a_2}\lambda_{AB}\Phi_{AB(h=h0)}e^{\frac{h0-h}{\lambda_{AB}}} \quad (8)$$

$$\Phi_{AB(h=h0)} = -\frac{K}{2\pi h_0 \lambda_{AB}} \quad (9)$$

$$\log K = -3.5(Cos\theta_1 + Cos\theta_2) - 18 \quad (10)$$

where V_{AB}: Lewis acid-base interaction potential energy (J), λ_{AB}: decay (Debye) length of water (m), $\Phi_{AB(h = h0)}$: Lewis acid-base free interaction potential energy between surfaces at contact (J m^{-2}), K: hydrophobic constant (J) θ_i: contact angle of surface i (°). And for a sphere and a plate [18]:

$$V_{AB} = 2\pi a\lambda_{AB}\Phi_{AB(h=h0)}e^{\frac{h0-h}{\lambda_{AB}}} \quad (11)$$

Particles that have superficial charges may be hydrated in a solution, and these water molecules will hinder the approximation to the mentioned surfaces. Then, the extra hydration repulsion energy origins when particles need to eliminate the adsorbed water molecules to be in direct contact between them, affecting aggregation. Hydration interaction energy diminishes exponentially with distance [21]:

$$V_H = \pi a N_A C_h C_e \lambda_{AB}^2 e^{-\frac{h}{\lambda_{AB}}} \quad (12)$$

where V_H: hydration interaction potential energy (J), N_A: Avogadro number, C_h: hydration constant (J), C_e: salt concentration (mol m^{-3}).

Therefore, the total interaction potential energy is obtained as the sum of:

$$V_{TOTAL} = V_{EDL} + V_{vdW} + V_{AB} + V_H \quad (13)$$

3. Materials and methods

Bacteriophage PP7 (ATCC 15692-B2) belongs to *Leviviridae* family, *Levivirus* genus and infects *Pseudomonas aeruginosa*. It is a naked virus, i.e. no enclosing envelope, has icosahedral capsid and consists of single-stranded RNA, surrounded by 180 copies of the coat protein, each 127 amino acid residues long. This coat protein contains 42% of hydrophobic residues. PP7 can be a surrogate for poliovirus in water treatment processes, since both are icosahedral and have similar diameter (25–30 nm) [12]. Besides, PP7 is non-infective to humans and easy to enumerate. It offers challenging conditions for membrane testing in virus filtration due to its small size [22] and was selected by the Parenteral Drug Association (PDA) as the viral model to test for small virus-retentive membrane-based filters [23].

Reagent grade, NaCl, $MgCl_2{\cdot}6H_2O$, $NaHCO_3$, $CaCl_2{\cdot}2H_2O$ (Anedra, Argentina) were employed. Solutions were prepared with Type I water (18 MΩ.cm). The nutrient broth (Britania, Argentina) was prepared mixing 8 g in 1 L of deionized water. The soft nutrient agar for bacteriophage titration was prepared mixing 8 g of nutrient broth and 7.5 g of agar–agar technical for microbiology (Merck, Germany) in 1 L of deionized water. The nutrient agar for Petri dishes was prepared mixing 8 g of nutrient broth, 8 g of NaCl and 15 g of agar–agar technical for microbiology in 1 L of deionized water. Materials and reagents were sterilized by autoclaving at 121 °C for 20 min. A modified polyethersulfone (PES) flat sheet ultrafiltration membrane was used (Pall Corp., USA). The molecular weight cut-off (MWCO), informed by the manufacturer, was 50 kDa. The average pore size was 0.067 μm determined by porosimetry, as previously reported [24].

3.1. Size and zeta potential measurements

First, the host bacteria *Pseudomonas aeruginosa* were incubated in nutrient broth for 24 h at 37 °C on an orbital shaker at 120 rpm. PP7 was then inoculated and incubated under the same conditions. Afterwards, the virus suspension was centrifuged at 1000 × *g* for 15 min and the supernatant filtered through a 0.22 μm PVDF membrane (Millipore GVW P02500). This suspension was dialyzed through a 100 kDa MWCO membrane (SpectraPor Biotech CE, Spectrum Laboratories, USA) twice: first, against water, and secondly, against the appropriate solution for 20 h each; afterwards this final suspension was again filtered and kept at 4 °C overnight before measuring the zeta potential and the hydrodynamic diameter [10]. Twelve different conditions of water chemistry were considered, composed of variable concentrations of NaCl, $NaHCO_3$, $CaCl_2$ and $MgCl_2$, to give for each salt levels of 1 mM, 10 mM and 100 mM ionic strength.

The concentration of each bacteriophage suspension was determined after the last filtration, with the double agar method. A plate containing only agar was incubated to discard bacterial contamination, serving as negative control for bacteria. A plate only seeded with bacteria served as negative control for bacteriophage. The plates were incubated at 37 °C for 24 h. The concentrations were between 6×10^7 and 7×10^8 PFU/ml.

The hydrodynamic diameter and the bacteriophage's zeta potential were measured by Dynamic Light Scattering (DLS) and laser Doppler micro electrophoresis respectively, using a Zetasizer Nano ZS (Malvern, UK) at 25 °C as described elsewhere [15,25].

The membrane surface zeta potential was obtained using a zeta potential accessory and a suspension of tracer particles in order to measure electro-osmosis near to the surface, from which membrane zeta potential can be derived [26].

3.2. Filtration experiments

The experimental set up consisted of a membrane filtration unit, connected to a feed tank through a peristaltic pump, a permeate tank on a scales, and control instruments (two pressure gauges and a flowmeter) (Fig. 1). The tangential-flow filtration system operated at a constant pressure of 0.3 bar and at room temperature (22–25 °C). No significant transmembrane flux decrease was observed during the filtration assays; neither significant increase of the temperature, therefore the dynamic viscosity of the solution did not change.

All components were sterilized prior to use and pH was measured but not modified. Synthetic aqueous matrixes, based on relevant environmental water qualities [27], were prepared mixing: $CaCl_2{\cdot}2H_2O$ (5.8 g/L), $MgCl_2{\cdot}6H_2O$ (5.9 g/L), $Ca(NO_3)_2{\cdot}4H_2O$ (3 g/L), $Mg(NO_3)_2{\cdot}6H_2O$ (3 g/L), $NaHCO_3$ (8.94 g/L) in deionized water, as published in a previous work [13].

The host bacteria in nutrient broth was inoculated with PP7 and incubated for 18 h at 37 °C. Afterwards, the viral suspension was centrifuged at 1000 × *g* for 5 min and the supernatant filtered through a 0.22 μm filter. The nucleic acids from each sample were extracted using QIAamp Viral RNA kit (Qiagen, Valencia, CA) according to the manufacturer's directions, with a final elution volume of 80 μL, and stored at −80 °C immediately after extraction until use. The cDNA was synthesized using the Superscript III Reverse Transcriptase kit (Invitrogen) following the manufacturer's instructions. For the quantitative detection of PP7, the concentrations of the bacteriophage suspensions were determined by qPCR (quantitative Polymerase Chain Reaction) by taking samples of the inlet, permeate and retentate, using

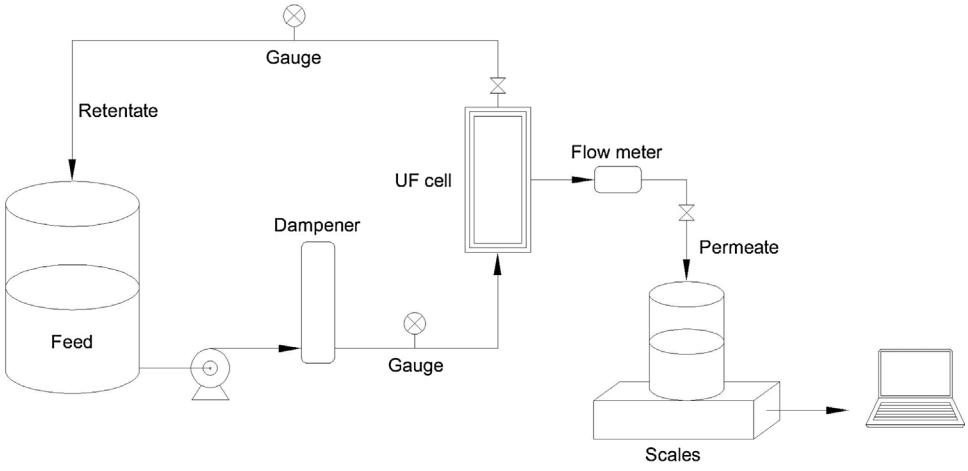

Fig. 1. Filtration experiments set up.

oligonucleotides previously validated and published were used under conditions described before [22]. The bacteriophage concentration in the feed was kept between 1.7×10^5 and 1.1×10^6 PFU/ml. We verified that the qPCR reactions were not affected by inhibition. All the analyses were performed by duplicate and positive and negative controls were carried out in simultaneous with the samples [13].

The viral removal efficiencies were calculated in terms of the log removal value (LRV) as:

$$LRV = -log\left(\frac{C_p}{C_f}\right) \quad (14)$$

where C_f and C_p are the virus concentrations (gene copy ml^{-1}) in the feed (f) and permeate flow (p), respectively.

3.3. DLVO and XDLVO

The bacteriophage PP7 was considered as a sphere due to its icosahedral shape [4] and the flat sheet membrane was regarded as an infinite plate. The Hamaker constants were: $A_{11} = 8.55 \times 10^{-20}$ J, $A_{22} = 7.45 \times 10^{-20}$ J, $A_{33} = 3.70 \times 10^{-20}$ J, $A_{131} = 1 \times 10^{-20}$ J, $A_{132} = 8.06 \times 10^{-21}$ J, which were derived from literature [21,28–30].

Assumed contact angle for the bacteriophage was 33° [18]. Measured contact angle of the membrane was 59.38° [24]. To calculate hydration repulsion we used $C_h = 1.6 \times 10^{-20}$ J and $\lambda_{AB} = 0.6$ nm [31] regarding the bacteriophage as a colloid with a protein capsid.

3.4. Statistical analysis

Effects of pH and salts at different ionic strengths on the viral particle size and the zeta potential of the membrane and the bacteriophage were compared using one-way Analysis of variance (ANOVA) and Tukey test post-hoc multiple-comparisons procedures. The DLVO modeling results were compared using Kruskal-Wallis, a non-parametric test. Analyses were performed using SigmaPlot v.12.5 (Systat Software, Inc.) and GraphPad Prism v.6.02 (GraphPad Software, Inc.) with a significance level of $\alpha = 0.05$.

4. Results and discussion

4.1. Bacteriophage size

The average hydrodynamic diameter of the bacteriophages suspended in the different water chemistries investigated ranged between 49.22 and 83.57 nm, which differs from the diameter of an isolate viral particle of around 27 nm reported in the literature [32]. For each ionic strength condition, the size was minimally affected by the pH ($p > 0.999$). Therefore, the average diameter in the pH range considered is indicated in Fig. 2. When in NaCl 10 and 100 mM, the variation according to pH was larger than with the other salts at the same ionic strengths. In $CaCl_2$ 1 mM ionic strength, the largest variation was obtained. And in $NaHCO_3$ at all ionic strength, the least variation.

Even though the largest average hydrodynamic diameter measured (83.57 ± 8.31 nm) was with $MgCl_2$ at 1 mM of ionic strength, that size indicates a low degree of aggregation among the viruses (maximum three particles) over the range of pH and ionic strengths tested. Therefore, minimal aggregation can be assumed when the ionic strength increased from 1 to 100 mM at pH above the isoelectric point (pI = 4.3–4.9) [33]. This finding is in agreement with Langlet et al., 2008 who worked with bacteriophages MS2 and Qβ and found isolate particles at pH above 7 at 1 mM to 100 mM of ionic strength [10]. Thus, the small aggregate state is prevalent among the viral particles at pH of environmental waters and therefore challenges the membrane to work in the worst-case scenario. A different outcome was reported for other viruses, e.g. GA phages, since they formed aggregates under the conditions investigated [10].

The hydrodynamic diameter is the diameter of a rigid hypothetical sphere which velocity of diffusion is the mean of the velocities of diffusion of its different spatial orientations. It is calculated from data of diffusion coefficients obtained by DLS [34]. Macromolecules are not rigid and spherical, but dynamic and they can interact with the solvent in which they are suspended. Therefore, the calculated diameter indicates the apparent size taking into consideration attraction and association with solvent molecules [35]. In the light of filtration membrane processes, the membrane cut-off accounts for the molecular weight but not for the tridimensional structure of the molecule. This is particularly important for proteins, bacteria and viruses, since their apparent size may change because of the water matrix chemistry [35].

The aggregation of viral particles is important when evaluating and comparing retention efficiencies of different membranes as to avoid overestimating removal. Perfectly disperse viral particles represents the most challenging scenario [10]. However, this condition can be obtained at pH values generally far from the pI and in low ionic strength solutions for some viruses; whereas in environmental waters many factors (such as pH, ionic strength, presence of colloids and organic matter) affect the ideal isolation state and aggregation occurs [13,36,37].

4.2. Bacteriophage and membrane zeta potentials

Zeta potentials for both phage and membrane surface were measured at 1, 10 and 100 mM ionic strength. pH was varied between 5 and 8 in order to mimic pH of natural waters [9] and its effect studied at all ionic strengths for the phage (Fig. S1–S3 in Supplementary material) and at 10 mM for the membrane (Fig. 3).

Zeta potential of the bacteriophage PP7 was always negative, between −44.63 and −10.53 mV (Fig. S1–S3 in Supplementary material). There was no significant change over the considered pH range for NaCl, $CaCl_2$ and $MgCl_2$ at the three ionic strengths tested. This fact is in agreement with previous modeling of the phage's surface charge at NaCl 100 mM [38], where this stability was predicted at pH 6 and higher. However, in the case of $NaHCO_3$ 1 mM there is a significant more negative zeta potential (-44.63 ± 2.80 mV) close to the neutral pH ($p < 0.001$) (Fig. S1 in Supplementary material).

In Table 1, it can be seen that there were statistically significant differences between the mean zeta potential measured when varying salt and ionic strength; conversely, $NaHCO_3$ 10 mM and 100 mM did not show any significant difference. Increasing ionic strength produced an increase in the zeta potential of the bacteriophage (less negative), as expected due to compression of the ionic double layer. In presence of monovalent cations, the viral particles showed more negative values at

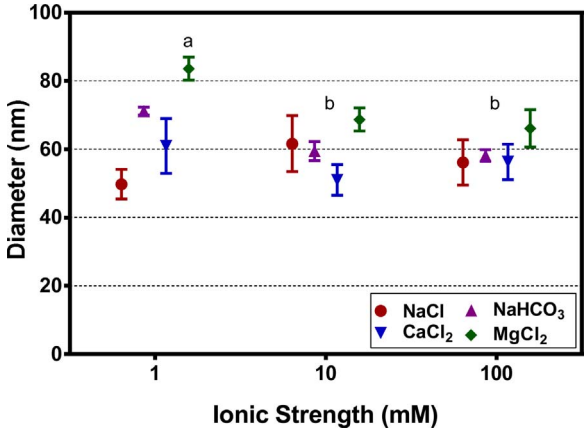

Fig. 2. Average hydrodynamic diameter of bacteriophage PP7 at different ionic strengths of tested salts. Letters denote results from Tukey's honestly significant post-hoc test for comparison of size at different ionic strengths. Different letters denote statistically significant difference between mean size measurements ($p < 0.05$).

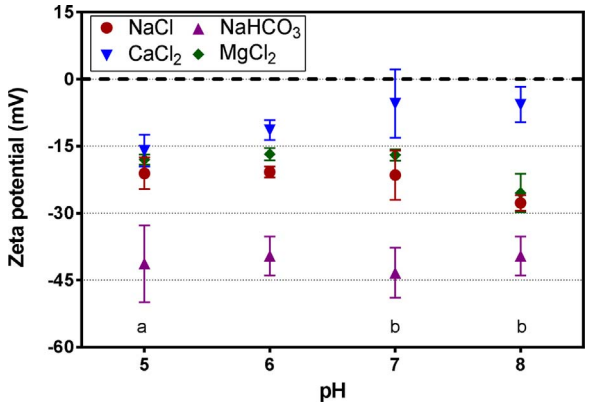

Fig. 3. Effect of pH on membrane zeta potential in tested salts solutions at 10 mM of ionic strength. Letters denote results from Tukey's honestly significant post-hoc test for comparison of zeta potential in $CaCl_2$ solutions at different pH levels. Different letters indicate statistically significant differences between groups ($p < 0.05$), values at pH 6 were not statistically different.

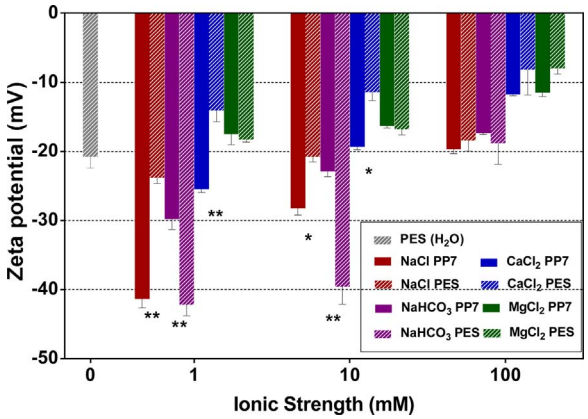

Fig. 4. Zeta potential of bacteriophage and membrane at different ionic strengths. pH was not modified (pH = 6 for NaCl, $NaHCO_3$ 1 mM, $CaCl_2$ and $MgCl_2$, pH = 8 for $NaHCO_3$ 10 mM and pH = 8.5 for $NaHCO_3$ 100 mM). Symbols indicate data sets that are statistically significant at different levels: * $p < 0.05$, ** $p < 0.01$.

each ionic strength; meanwhile in $MgCl_2$ the zeta potential was always less negative (> -20 mV) indicating less stability of the particles. At the lowest ionic strength (1 mM), the zeta potential was more negative than −25 mV for all salts besides $MgCl_2$. In all cases the pH of the viral suspensions was not modified, that is 6 for NaCl, $NaHCO_3$ 1 mM, $CaCl_2$ and $MgCl_2$, 8 for $NaHCO_3$ 10 mM and 8.5 for $NaHCO_3$ 100 mM.

The flat membrane showed negative values at a constant ionic strength of 10 mM and was not influenced by the pH in the studied range (Fig. 3), except for $CaCl_2$. In the presence of $CaCl_2$ ion adsorption took place neutralizing part of the surface charge and turning it less negative as pH was increased, in this way the membrane was significantly more negative (−16.0 ± 3.56 mV) at pH 5 compared to pH 7 (−5.48 ± 7.72 mV) and 8 (−5.71 ± 3.97 mV) ($p = 0.0273$ and $p = 0.0319$, respectively). Calcium cations specifically adsorb to the membrane surface, neutralizing the negative charges that would arise at basic pH and decreasing the absolute value of the zeta potential. At high pH values, these cations led to low electrical double layer repulsive interactions and attractive van der Waals interactions prevailed.

The zeta potential was significantly different among the salts tested. However, similar average values over the evaluated pH where measured in NaCl (−22.78 ± 3.29 mV) and $MgCl_2$ (−19.33 ± 4.15 mV) ($p = 0.322$). $NaHCO_3$ showed the most negative value with a mean of −40.98 ± 1.80 mV, and $CaCl_2$ the less negative, −9.65 ± 5.043 mV (Fig. 3).

The zeta potential of the PES membrane was −20.8 ± 2.82 mV in Type I water and in presence of NaCl showed similar charge, which varied between −23.8 and −18.4 mV, at all ionic strengths at constant pH ($p = 0.178$). Similarly, no different charge on the membrane surface was observed in $NaHCO_3$ 100 mM ($p = 0.5943$), and $MgCl_2$ 10 mM ionic strength ($p = 0.1004$). The membrane was significantly more negative in $NaHCO_3$ 1 and 10 mM ($p = 0.0007$ and $p = 0.0033$, respectively) and less negative in $CaCl_2$ 1 mM ($p = 0.0421$), 10 mM ($p = 0.0.0108$), 100 mM ($p = 0.0351$), and in $MgCl_2$ 1 mM ($p = 0.0089$) and 100 mM ($p = 0.0021$) (Fig. 4).

The membrane was significantly less negatively charged than the virus for the case of NaCl 1 ($p < 0.0001$) and 10 mM ($p = 0.043$), and $CaCl_2$ 1 ($p = 0.0021$) and 10 mM of ionic strength ($p = 0.0163$). The virus was statistically significant less negatively charged than the membrane when in $NaHCO_3$ 10 mM ionic strength ($p < 0.0001$). Both, membrane and virus, had approximately the same charge (no significant difference) at 1 mM ionic strength of $NaHCO_3$ ($p = 0.9835$) and $MgCl_2$ ($p = 0.9197$), at 10 mM of $MgCl_2$ ($p > 0.9999$), and at 100 mM of NaCl ($p > 0.999$), $NaHCO_3$ ($p = 0.9996$), $CaCl_2$ ($p = 0.8367$) and $MgCl_2$ ($p = 0.9789$) (Fig. 4).

Two functional groups are present in the PES structure, the hydrophilic sulfonil group and the hydrophobic benzene ring. The metallic cations interact, completely or partially, with the negative atomic fractions of the membrane; being the most probable interaction sites the two O-atoms ligated to S in the sulfonil group [39]. Therefore, the membrane can be neutralized and the addition of cations might increase the attraction of viral particles. Thus, motion through the pores is facilitated and viral removal is decreased.

4.3. Filtration results

Ultrafiltration of bacteriophage PP7 was performed using a PES membrane (MWCO 50 kDa) as previously described [13]. Logarithmic Removal Values (LRV) varied between 1.50 and 2.83 (Table 2).

The least removal was obtained when Mg^{2+} and Ca^{2+} were present at the highest concentration, along with an elevated concentration of chloride (double to the cations concentrations). These cations have the largest hydrated radius (Na^+: 0.4 nm, Ca^{2+}: 0.6 nm, Mg^{2+}: 0.8 nm) [40] and adsorption or proximity to the negatively charged membrane can act as bond between the virus and the surface leading to a low

Table 1
Zeta potential of bacteriophage PP7 at different salts and ionic strengths.

Salts	PP7 Zeta potential (mean ± SD)			p-values		
	Ionic Strength					
	1 mM	10 mM	100 mM	1 mM vs 10 mM	1 mM vs 100 mM	10 mM vs 100 mM
NaCl	−41.333 ± 2.250	−28.333 ± 1.650	−19.700 ± 1.081	< 0.0001	< 0.0001	< 0.0001
$NaHCO_3$	−29.800 ± 2.587	−22.900 ± 1.345	−17.333 ± 0.379	< 0.0001	< 0.0001	0.0004
$CaCl_2$	−25.467 ± 0.850	−19.133 ± 0.709	−11.800 ± 0.346	< 0.0001	< 0.0001	< 0.0001
$MgCl_2$	−17.500 ± 2.646	−16.333 ± 0.503	−11.500 ± 0.917	0.6135	0.0002	0.0017

SD: Standard deviation.

Table 2
Bacteriophage PP7 removal (LRV) by PES membrane filtration of aqueous matrices with different ionic strength.

Ionic strength				LRV
Na^+	HCO_3^-	Ca^{2+}	Mg^{2+}	
high (1.23 mM)	high (1.23 mM)	low (0.55 mM)	low (0.41 mM)	2.83
low (0.41 mM)	low (0.41 mM)	high (2.50 mM)	low (0.41 mM)	1.53
low (0.41 mM)	low (0.41 mM)	low (0.55 mM)	high (1.24 mM)	1.50

removal.

The highest removal was when Na^+ and HCO_3^- together were the dominant species. The presence of an indifferent ion such as Na^+ suggested the electrostatic nature.

4.4. DLVO and XDLVO analysis

Attachment of viruses to surfaces is generally due to electrostatic interactions [41]. The van der Waals potential energies are constant for two given surfaces for all water matrixes, since they depend on the geometry and on properties of the interacting macroscopic bodies and of the medium. The electrical double layer potential energies for two given surfaces change as function of the solution ionic strength and the zeta potential of both bacteriophage and membrane. Lewis acid-base and hydration repulsion energies were calculated and incorporated to the total interaction potential energy, though they could be neglected if compared to DLVO interactions. In addition, it must be stated that different reported contact angles for viruses (96° and 42° from [42]) were also tried and this assumption did not alter the conclusions due to the minor relevance of Lewis acid-base forces compared to van der Waals and electrical double layer interactions.

4.5. DLVO analysis of viral particle stability

Interaction potential energies were analyzed for the bacteriophages in different background solutions (Fig. S4–S6 in Supplementary material). An energy barrier preventing aggregation was predicted in all cases except for solutions containing divalent cations at 100 mM of ionic strength (Fig. S6 in Supplementary material). This barrier was smaller with increasing ionic strength.

DLVO modeling was also made for interactions under variable pH and all ionic strengths. The total interactions did not show significant differences since the variations of zeta potentials were very small. The analysis suggests that pH would not affect the stability of viral aggregates which agreed with experimental observations.

4.6. DLVO analysis of virus-membrane interactions

Interaction potential energies were analyzed for the bacteriophage and the membrane in different background solutions (Fig. 5 and Fig. S7 and S8 in Supplementary material). Net attraction forces were predicted for the highest ionic strength condition (100 mM) for $CaCl_2$ and $MgCl_2$ (Fig. S8 in Supplementary material). Low energy barriers were obtained (3.5 to 5 k T) for NaCl and $NaHCO_3$ at 100 mM, not expected to prevent attachment to the membrane (Fig. S8 in Supplementary material). For all other background solutions (1 and 10 mM), energy barriers were obtained and electrostatic repulsion expected (Fig. 5 and Fig. S7 in Supplementary material). In solutions of $CaCl_2$ and $MgCl_2$ the interaction potential energies showed similar behaviors at all ionic strengths tested ($p > 0.05$).

Since both virus and membrane were negatively charged, high removal rates would be expected due to electrostatic repulsion and therefore, viruses will not reach and attach to the membrane surface, but remain in the retentate. Moreover, the membrane average pore diameter of 67 nm makes size exclusion an important mechanism for removal in natural waters where viruses are not usually present as individual particles but small aggregates [8].

The ionic strength used in each ultrafiltration experiment was very close to or barely exceeded 1 mM, therefore DLVO plus XDLVO modeling for 1 mM solutions was applied to its interpretation (Fig. 5). The highest energy barriers corresponded to $NaHCO_3$ and NaCl giving rise to repulsion which enhanced the effectiveness of filtration. Lesser values were obtained for divalent cations. The presence of Ca^{2+} and Mg^{2+} reduced the repulsion but in turn, prevented attachment to the membrane due to the enhanced hydrated radius. Filtration removal rates were expected to be reduced, as observed experimentally (Table 2).

The highest removal rate was obtained when an indifferent cation such as Na^+ was dominant, which indicated the importance of electrostatic forces in the filtration. Coincidently, DLVO calculations showed the highest energy barriers confirming this assumption. The difference in surface charge of the bacteriophage and the membrane was larger when Na^+ was present in the solution (Fig. 4, at 1 mM ionic strength), which made the repulsive forces more important. Consequently, viruses were effectively repelled from the membrane surface and LRV was enhanced. The removal increased in the same way that energy barriers predicted by DLVO, showing the importance of electrostatic interactions in virus removal by ultrafiltration.

Modeling predicted no significant changes when varying pH at 10 mM ionic strength. In all cases, energy barriers prevailed, due to the small variation in zeta potentials with pH.

Some limitations to the modeling arise from the fact that viruses are not perfect, rigid spheres with homogeneous surface, but soft particles

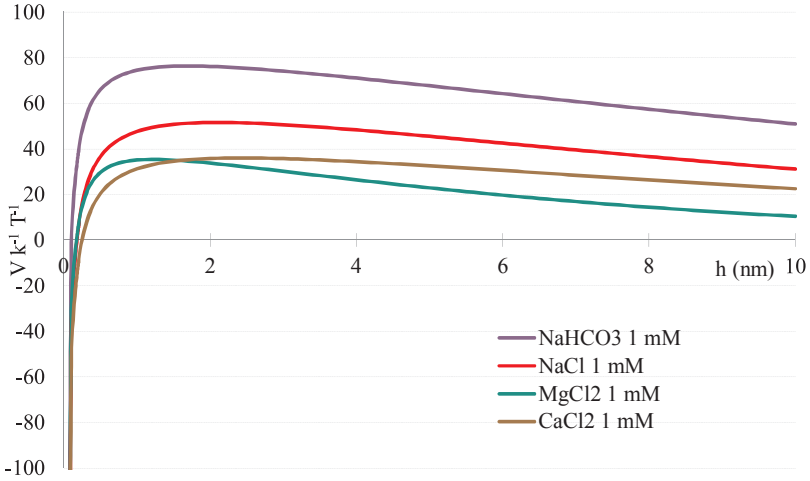

Fig. 5. Predicted interaction potential energies for a particle of bacteriophage and PES membrane at 1 mM ionic strength.

where the surface is not clearly defined and electrolyte ions can penetrate it [43]. Therefore, the electrical double layer is not limited to the outside of the virus but develops within the surface charge layer and the zeta potential importance and meaning may be questioned [44]. Moreover, commercial PES membrane surfaces are not perfectly smooth and homogenous as assumed in DLVO calculations.

5. Conclusions

Ultrafiltration to disinfect waters proved to be efficient, but the process was affected by the aqueous matrix and therefore, partial removal of PP7 was obtained. The presence of divalent cations diminished the effectiveness as opposed to monovalent cations and species with amphoteric behavior such as bicarbonate. Size of the bacteriophage did not vary considerably with pH or ionic strength. Furthermore, at pH of environmental waters (5 to 8) viruses form small aggregates, challenging membrane-based disinfection treatments. DLVO and XDLVO modeling of interactions between PP7 particles predicted stability for the whole range of studied conditions, as it was confirmed by DLS measurements. Low energy barriers were obtained for NaCl and $NaHCO_3$ at 100 mM. For 1 and 10 mM background solutions, electrostatic repulsion was expected. The viral removal increased in the following order: Mg^{2+}, Ca^{2+}, and Na^+ with HCO_3^-. The same trend was observed for the height of the energy barriers predicted by the modeling. For bacteriophage PP7, changes in pH ranged between 5 and 8 (far from the virus isoelectric point) or ionic strength did not alter the modeling predictions regarding stability and attachment. These results highlighted the importance of electrostatic repulsion in enhancing virus removal by membrane filtration.

The importance of these results in practical applications lies in the fact that special care needs to be taken when designing a filtration scheme to remove small microorganisms such as viruses. It is of vital importance to take into consideration the composition of the aqueous matrix since it affects the process efficiency. Interactions between the membrane material and the outer surface of the viral particle are also of great importance since the electrostatic nature of the process is key to achieve safe waters. Experimental tests confirmed DLVO predictions that electrostatic forces in presence of divalent cations hinder the performance of the filtration to a satisfactory level. In particular, viruses act like charged particles and the surface of the membrane should be selected or designed as to maximize the repulsion that will arise in the filtration unit.

Appendix A. Supplementary data

Supplementary data associated with this article can be found, in the online version, at https://doi.org/10.1016/j.jece.2017.11.041.

References

[1] M.A. Borchardt, S.K. Spencer, B.A. Kieke, E. Lambertini, F.J. Loge, Viruses in nondisinfected drinking water from municipal wells and community incidence of acute gastrointestinal illness, Environ. Health Perspect. 120 (2012) 1272–1279.

[2] A.H. Havelaar, M. van Olphen, Y.C. Drost, F-specific RNA bacteriophages are adequate model organisms for enteric viruses in fresh water, Appl. Environ. Microbiol. 59 (1993) 2956–2962.

[3] J.L. Melnick, C.P. Gerba, G. Berg, The ecology of enteroviruses in natural waters, Crit. Rev. Env. Cont. 10 (1980) 65–93.

[4] A.M. ElHadidy, S. Peldszus, M.I. Van Dyke, An evaluation of virus removal mechanisms by ultrafiltration membranes using MS2 and φX174 bacteriophage, Sep. Purif. Technol. 120 (2013) 215–223.

[5] K. Kreissel, M. Bosl, P. Lipp, M. Franzreb, B. Hambsch, Study on the removal efficiency of UF membranes using bacteriophages in bench-scale and semi-technical scale, Water Sci. Technol. 66 (2012) 1195–1202.

[6] L. Fiksdal, T. Leiknes, The effect of coagulation with MF/UF membrane filtration for the removal of virus in drinking water, J. Membr. Sci. 279 (2006) 364–371.

[7] S.R. Farrah, C.P. Gerba, C. Wallis, J.L. Melnick, Concentration of viruses from large volumes of tap water using pleated membrane filters, Appl. Environ. Microbiol. 31 (1976) 221–226.

[8] J.G. Jacangelo, S.S. Adham, J.M. Laine, Mechanism of cryptosporidium giardia, and MS2 virus removal by MF and UF, J. Am. Water Works Assoc. 87 (1995) 107–121.

[9] R.M. Chaudhry, R.W. Holloway, T.Y. Cath, K.L. Nelson, Impact of virus surface characteristics on removal mechanisms within membrane bioreactors, Water Res. 84 (2015) 144–152.

[10] J. Langlet, F. Gaboriaud, J.F.L. Duval, C. Gantzer, Aggregation and surface properties of F-specific RNA phages: implication for membrane filtration processes, Water Res. 42 (2008) 2769–2777.

[11] W.O.K. Grabow, Bacteriophages Update on application as models for viruses in water, Water SA 27 (2001) 251–268.

[12] K.H. Oshima, T.T. Evans-Strickfaden, A.K. Highsmith, E.W. Ades, The use of a microporous polyvinylidene fluoride (PVDF) membrane filter to separate contaminating viral particles from biologically important proteins, Biologicals 24 (1996) 137–145.

[13] M.C. Cruz, L.C. Romero, M.S. Vicente, V.B. Rajal, Statistical approaches to understanding the impact of matrix composition on the disinfection of water by ultrafiltration, Chem. Eng. J. 316 (2017) 305–314.

[14] C. Shen, M.S. Phanikumar, T.T. Fong, I. Aslam, S.P. McElmurry, S.L. Molloy, J.B. Rose, Evaluating bacteriophage P22 as a tracer in a complex surface water system: the grand river michigan, environ, Sci. Technol. 42 (2008) 2426–2431.

[15] M.M. Fidalgo de Cortalezzi, M.V. Gallardo, F. Yrazu, G.J. Gentile, O. Opezzo, R. Pizarro, H.R. Poma, V.B. Rajal, Virus removal by iron oxide ceramic membranes, J. Environ. Chem. Eng. 2 (2014) 1831–1840.

[16] J.S. Meschke, M.D. Sobsey, Comparative adsorption of Norwalk virus, poliovirus 1 and F+ RNA coliphage MS2 to soils suspended in treated wastewater, Water Sci. Technol. 38 (1998) 187–189.

[17] H. Huang, T.A. Young, K.J. Schwab, J.G. Jacangelo, Mechanisms of virus removal from secondary wastewater effluent by low pressure membrane filtration, J. Membr. Sci. 409–410 (2012) 1–8.

[18] C.V. Chrysikopoulos, V.I. Syngouna, Attachment of bacteriophages MS2 and (X174 onto kaolinite and montmorillonite: extended-DLVO interactions, Colloid Surf. B 92 (2012) 74–83.

[19] B. Derjaguin, L. Landau, Theory of the stability of strongly charged lyophobic sols and of the adhesion of strongly charged particles in solutions of electrolytes, Acta Physicochim. URSS 14 (1941) 733–762.

[20] E.J.W. Verwey, J.T.G. Overbeek, Theory of the stability of lyophobic colloids, J. Colloid Sci. 10 (1955) 224–225.

[21] M. Elimelech, J. Gregory, X. Jia, R.A. Williams, J. Gregory, X. Jia, R.A. Williams, Particle Deposition & Butterworth-Heinemann Woburn Aggregation, (1995).

[22] V.B. Rajal, B.S. McSwain, D.E. Thompson, C.M. Leutenegger, B.J. Kildare, S. Wuertz, Validation of hollow fiber ultrafiltration and real-time PCR using bacteriophage PP7 as surrogate for the quantification of viruses from water samples, Water Res. 41 (2007) 1411–1422.

[23] S. Lute, W. Riordan, L.F. Pease 3rd, D.H. Tsai, R. Levy, M. Haque, J. Martin, I. Moroe, T. Sato, M. Morgan, M. Krishnan, J. Campbell, P. Genest, S. Dolan, K. Tarrach, A. Meyer, M.R. Zachariah, M.J. Tarlov, L.M. Etze, K. Brorson, H. Aranha, M. Bailey, J. Bender, J. Carter, Q. Chen, C. Dowd, R. Jani, D. Jen, S. Kidd, T. Meltzer, K. Remington, I. Rice, C. Romero, M. Jornitz, C.M. Sekura, G. Sofer, R. Specht, P. Wojciechowski, A consensus rating method for small virus-retentive filters. I. Method development, PDA J. Pharm. Sci. Technol. 62 (2008) 318–333.

[24] M.C. Cruz, G. Ruano, M. Wolf, D. Hecker, E. Castro Vidaurre, R. Schmittgens, V.B. Rajal, Plasma deposition of silver nanoparticles on ultrafiltration membranes: antibacterial and anti-biofouling properties, Chem. Eng. Res. Des. 94 (2015) 524–537.

[25] G.J. Gentile, M.M. Fidalgo de Cortalezzi, Enhanced retention of bacteria by TiO2 nanoparticles in saturated porous media, J. Contam. Hydrol. 191 (2016) 66–75.

[26] J.C.W. Corbett, F. McNeil-Watson, R.O. Jack, M. Howarth, Measuring surface zeta potential using phase analysis light scattering in a simple dip cell arrangement, Colloid Surf. A 396 (2012) 169–176.

[27] M.C. Cruz, D.G. Cacciabue, J.F. Gil, O. Gamboni, M.S. Vicente, S. Wuertz, E. Gonzo, V.B. Rajal, The impact of point source pollution on shallow groundwater used for human consumption in a threshold country, J. Environ. Monit. 14 (2012) 2338–2349.

[28] S. Kang, E.M.V. Hoek, H. Choi, H. Shin, Effect of membrane surface properties during the fast evaluation of cell attachment, Sep. Sci. Technol. 41 (2006) 1475–1487.

[29] T.K. Tokunaga, Physicochemical controls on adsorbed water film thickness in unsaturated geological media, Water Resour. Res. 47 (2011).

[30] F.L. Leite, C.C. Bueno, A.L. Da Róz, E.C. Ziemath, O.N. Oliveira, Theoretical models for surface forces and adhesion and their measurement using atomic force microscopy, Int. J. Mol. Sci. 13 (2012) 12773–12856.

[31] J.A. Molina-Bolívar, J.L. Ortega-Vinuesa, How proteins stabilize colloidal particles by means of hydration forces, Langmuir 15 (1999) 2644–2653.

[32] J. Rumnieks, K. Tars, Diversity of pili-specific bacteriophages: genome sequence of IncM plasmid-dependent RNA phage M, BMC Microbiol. 12 (2012) 1–8.

[33] K. Brorson, H. Shen, S. Lute, J.S. Pérez, D.D. Frey, Characterization and purification of bacteriophages using chromatofocusing, J. Chromatogr. A 1207 (2008) 110–121.

[34] Malvern, Zetasizer Nano Series User Manual, Malvern Instruments Ltd., Worcestershire, U.K, 2007.

[35] J.A.D.L. Rios, J. Sahuquillo, M.A. Merino, M.A. Poca, L. Expósito, Microdiálisis de alta resolución: aspectos metodológicos y aplicación al estudio de la respuesta inflamatoria cerebral, Neurocirugía 20 (2009) 433–448.

[36] A. Furiga, G. Pierre, M. Glories, P. Aimar, C. Roques, C. Causserand, M. Berge, Effects of ionic strength on bacteriophage MS2 behavior and their implications for the assessment of virus retention by ultrafiltration membranes, Appl. Environ. Microbiol. 77 (2011) 229–236.

[37] M.A. Nascimento, M.E. Magri, C.D. Schissi, C.R. Barardi, Recombinant adenovirus as a model to evaluate the efficiency of free chlorine disinfection in filtered water samples, Virol. J. 12 (2015) 30.
[38] Rikkert J. Nap, Anže L. Božič, I. Szleifer, R. Podgornik, The role of solution conditions in the bacteriophage PP7 capsid charge regulation, Biophys. J. 107 (2014) 1970–1979.
[39] W.-Y. Ahn, A.G. Kalinichev, M.M. Clark, Effects of background cations on the fouling of polyethersulfone membranes by natural organic matter: experimental and molecular modeling study, J. Membr. Sci. 309 (2008) 128–140.
[40] J. Kielland, Effective diameters of unhydrated and hydrated ions, J. Am. Chem. Soc. 59 (1937) 1675–1678.
[41] N. Tufenkji, Modeling microbial transport in porous media: traditional approaches and recent developments, Adv. Water Resour. 30 (2007) 1455–1469.
[42] R. Attinti, J. Wei, K. Kniel, J.T. Sims, Y. Jin, Virus' (MS2, ϕX174, and aichi) attachment on sand measured by atomic force microscopy and their transport through sand columns, Environ. Sci. Technol. 44 (2010) 2426–2432.
[43] H. Ohshima, Electrokinetic phenomena of soft particles, Curr. Opin. Colloid Interface Sci. 18 (2013) 73–82.
[44] V.I. Syngouna, C.V. Chrysikopoulos, Cotransport of clay colloids and viruses in water saturated porous media, Colloid Surf. A 416 (2013) 56–65.